

Original Article

Osseous cyst-like lesions in the feet of lame horses: Diagnosis by standing low-field magnetic resonance imaging

T. S. MAIR* AND C. E. SHERLOCK†

Bell Equine Veterinary Clinic, Mereworth, Maidstone, Kent ME18 5GS, UK.

Keywords: horse;

Introduction

Although the medial condyle of the distal femur is the most common site of osseous cyst-like lesions (OCLLs) in horses, they are also recognised in a variety of other locations, including the phalanges (Pettersson and Sevelius 1968; Wagner *et al.* 1982; Haack *et al.* 1988; McIlwraith 1990; Scott *et al.* 1991; Dowling *et al.* 1998; Story and Bramlage 2004). These lesions are associated with varying degrees of lameness, and in some cases they can be incidental findings (McIlwraith 1990; Howard *et al.* 1995; Baxter 1996; Dyson *et al.* 2005). The diagnosis is usually achieved by radiography, with the lesions typically appearing as solitary, circular or semicircular lucent areas of bone (usually the subchondral bone), often surrounded by a sclerotic rim (Verschooten and DeMoor 1982; Dyson 2003). They are most commonly unicameral (single chambered), although bicameral and multicameral cysts can also occur (Butler *et al.* 2000). Sometimes, they have a neck that connects the cyst to the articular surface. The aetiology of these bone cysts is unknown, but is probably multifactorial, and may include trauma, developmental abnormalities (osteocondrosis), sepsis and ischaemia. OCLLs most commonly arise in the subchondral bone of the main weightbearing surface, but they have also been identified in the distal phalanx at the site of insertion of the collateral ligament of the distal interphalangeal (DIP) joint in association with desmitis of this ligament (Dyson 1998; McDiarmid 1998; Dyson *et al.* 2004; Smith *et al.* 2005).

Although OCLLs are generally diagnosed by radiography, in some cases they can be difficult to detect (Watkins 1999; Dyson *et al.* 2004; Garcia-Lopez and Kirker-Head 2004; Jacquet *et al.* 2007). In 2 horses with OCLLs associated with desmitis of the collateral ligaments of the DIP joint reported by Dyson *et al.* (2004), the OCLLs were not detected by standard radiographic views of the distal phalanx, but were identified by magnetic resonance (MR) imaging. OCLLs have been

identified by both high- (Dyson *et al.* 2004, 2005; Zubrod *et al.* 2004) and low-field MR imaging (Mitchell *et al.* 2006); however, few specific details of the MR characteristics were given in these reports.

This report describes the low-field MR imaging findings in 9 horses with foot lameness where OCLLs were identified within the hoof capsule in either the middle or distal phalanges. In each case the MR examination was performed in the standing horse, and the OCLLs were not detected by standard radiographic views of the feet prior to the MR imaging.

Materials and methods

The records of all horses undergoing standing MR examination as part of the evaluation of foot lameness at Bell Equine Veterinary Clinic over the 18 month period between July 2005 and December 2006 were reviewed. MR imaging was undertaken in the horses if they were affected by an unexplained lameness that had been demonstrated to originate from the foot using regional analgesia (palmar/plantar digital nerve block, abaxial sesamoid nerve block and/or intra-articular analgesia of the distal interphalangeal joint). Improvement in lameness score by at least 60% following regional analgesia was considered significant. Standard radiographic views were obtained in all horses prior to undergoing MR imaging. These included: lateromedial, weightbearing dorsopalmar or dorsoplantar, dorsoproximal-palmarodistal or dorsoproximal-plantarodistal oblique, and palmaroproximal-palmarodistal or plantaroproximal-plantarodistal oblique views (Butler *et al.* 2000). MR images were obtained under standing sedation using a 0.27 Tesla open magnet and dedicated extremity radio frequency coil¹ as described previously (Mair *et al.* 2005; Sherlock *et al.* 2007). MR images were obtained in sagittal, transverse and frontal planes using gradient echo (GRE) T1-weighted, GRE T2*-weighted and fast spin echo (FSE) short tau inversion recovery (STIR) sequences (**Table 1**). Images (both MR and radiographic) were routinely obtained of both front feet (or both hind feet in horses with hindlimb lameness).

*Author to whom correspondence should be addressed. †Present address: University of Georgia, College of Veterinary Medicine, Athens, Georgia 30602-7385, USA.

TABLE 1: MR imaging sequences used for imaging the equine digit

Sequence	TR	TE	Flip angle	TI	Slice thickness (mm)	Gap (mm)	Scan time (min)
STIR FSE	1800	28	90	80	5	0.5	5:01
T1W 3D GRE	23	7	40	N/A	2.5	0	2:30
T1W 2D GRE	97	8	80	N/A	5	0.5	4:15
T2*W 3D GRE	34	13	22	N/A	2.5	0	3:31
T2*W 2D GRE	130	13	30	N/A	5	0.5	5:23

TR = repetition time, TE = echo time, TI = inversion time, GRE = gradient echo, FSE = fast spin echo, STIR = short tau inversion recovery.

Horses were included in this study if no specific diagnosis accounting for the lameness was reached following routine evaluation of the radiographs, and an OCLL was identified in either the middle or distal phalanx by MR imaging. Cases where an OCLL was diagnosed by radiography prior to MR imaging were excluded. Cases where cyst-like lesions in the distal sesamoid (navicular) bone were diagnosed were also excluded.

The case details, history and diagnostic work-up of each horse were recorded. The MR features were recorded. Following diagnosis of an OCLL, the original radiographs were re-evaluated. Further radiographic views (using computed radiography - Fujifilm FCR XG-1)² were obtained following MR imaging in all cases, including lesion-oriented views (such as flexed dorsal 60° lateral-palmaromedial oblique and dorsal 60° medial-palmarolateral oblique views) based on the position of the OCLL diagnosed by MR imaging. The further radiographic studies were all performed within 4 weeks of the original studies.

Results

Nine horses met the inclusion criteria. These horses represented 3.5% of the total with unexplained foot lameness that underwent MR imaging during the study period. Details of the horses, affected limbs, severity and duration of lameness, and sites of the OCLLs are summarised in **Table 2**. All of the horses

were mature (age range 6–17 years), and most (6/9) were used for general riding activities. The duration of lameness ranged from one month to one year. Eight of the 9 horses were forelimb lame (bilateral forelimb lameness in 5 horses) and one was unilaterally hindlimb lame. The severity of the lameness (when trotted in a straight line) at the time of examination ranged from 1/10 to 8/10 (where 0/10 represents nonlameness and 10/10 represents nonweightbearing lameness).

OCLLs were diagnosed in 12 feet. These included 6 feet in 3 bilaterally lame horses, 2 feet in 2 bilaterally lame horses (in both cases the OCLL was present in the lamest limb), and 4 feet in 4 unilaterally lame horses. In the unilaterally lame horses, OCLLs were only identified in the lame limbs. In the 2 horses with bilateral lameness where an OCLL was found in only one foot (Cases 2 and 9), the contralateral foot had significant MR abnormalities, including evidence of desmitis of the collateral ligaments of the DIP joint in both cases. The site of the OCLLs included the distal phalanx in 11 feet (subchondral bone in 4 feet, insertion of one of the collateral ligaments of the DIP joint in 4 feet, and insertion of the distal sesamoidean impar ligament in 3 feet) (**Figs 1–3**) and the subchondral bone of the distal aspect of the middle phalanx in one foot (**Fig 4**).

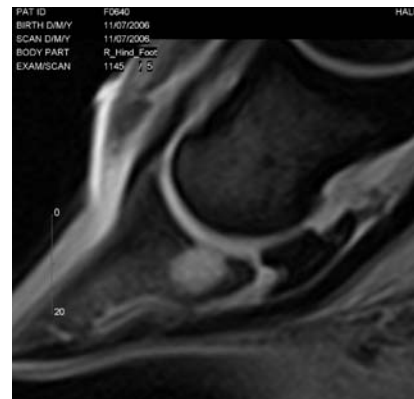


Fig 1a: Case 6. Sagittal GRE T2*-weighted image of the right hind foot showing a high signal subchondral OCLL in the distal phalanx.

TABLE 2: Details of horses diagnosed with OCLLs by standing low-field MR imaging

Case No.	Age (years)	Breed	Sex	Use	Affected limb(s)	Duration of lameness (months)	Lameness grade (of 10)	Site of OCLL
1	14	WB	F	G	RF	3	3	DP. Insertion of DSIL
2	6	TB	G	D,S	LF and RF	3	3	MP (LF). Subchondral
3	10	X	G	G	LF and RF	4	4	DP (LF and RF). Insertion of CL
4	10	X	F	G	LF and RF	10	6	DP (LF and RF). Insertion of DSIL
5	17	X	G	G	LF	4	1	DP. Subchondral
6	11	C	G	G	RH	1	8	DP. Subchondral
7	12	X	F	S	RF	9	2	DP. Insertion of CL
8	11	C	G	G	LF and RF	4	2	DP (LF and RF). Subchondral
9	8	X	F	E	LF and RF	12	2	DP (LF). Insertion of CL

Breed: WB = Warmblood, TB = Thoroughbred, X = crossbred, C = cob. Sex: F = female, G = gelding. Use: G = general riding, D = dressage, S = showjumping, E = eventing. RF = right fore, LF = left fore, RH = right hind. Lameness grade in straight line at the time of examination (most severely affected limb in bilaterally lame cases): scale of 0 (nonlame) to 10 (nonweightbearing lameness). Site of OCLL: DP = distal phalanx, MP = middle phalanx, DSIL = distal sesamoidean impar ligament, CL = collateral ligament of DIP joint.

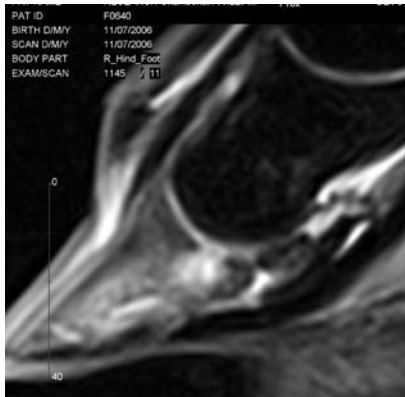


Fig 1b: Case 6. Sagittal STIR image of the right hind foot showing a high signal subchondral OCLL in the distal phalanx.

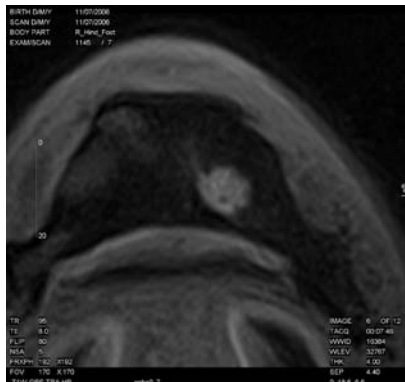


Fig 1c: Case 6. Transverse GRE T1-weighted image of the right hind foot showing a high signal subchondral OCLL in the distal phalanx.

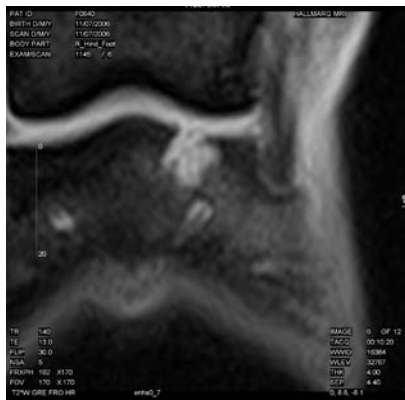


Fig 1d: Case 6. Frontal (dorsal) GRE T2*-weighted image of the right hind foot showing a high signal subchondral OCLL in the distal phalanx.

OCLLs were characterised by discrete, spherical or elliptical focal areas of high or intermediate signal within the bone in all sequences (i.e. GRE T1- and T2*-weighted images and STIR sequences). In most cases (8/12) the hyperintense lesion was surrounded by an area of bone with abnormally low signal in both GRE T1-weighted and STIR sequences (compared to the normal appearance of the trabecular bone), suggestive of osseous sclerosis (**Fig 4**). In all of the OCLLs

occurring in the subchondral bone adjacent to the DIP joint, the cyst appeared to involve or connect to the articular cartilage (**Figs 1** and **4**).

The major concurrent MR imaging findings (in addition to the OCLLs) in the 9 horses are summarised in **Table 3**. In all

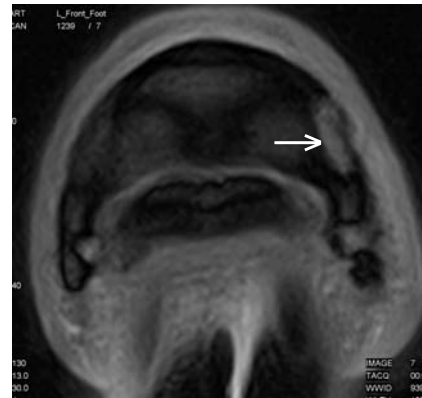


Fig 2a: Case 3. Transverse GRE T2*-weighted image of the left fore foot showing a high signal subchondral OCLL (arrow) in the distal phalanx at the insertion of the lateral collateral ligament of the DIP joint.

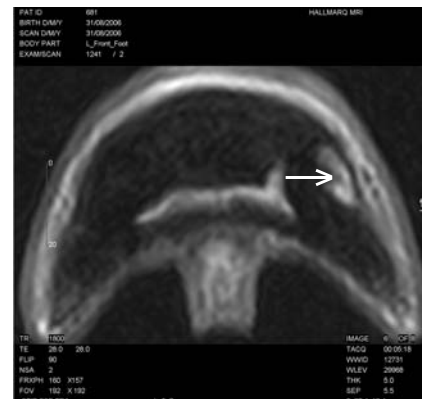


Fig 2b: Case 3. Transverse STIR image of the left fore foot showing a high signal subchondral OCLL (arrow) in the distal phalanx at the insertion of the lateral collateral ligament of the DIP joint.



Fig 2c: Case 3. Frontal (dorsal) GRE T2*-weighted image of the left fore foot showing a high signal subchondral OCLL (arrow) in the distal phalanx at the insertion of the lateral collateral ligament of the DIP joint.

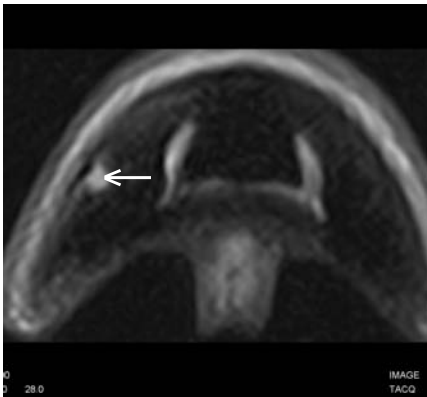


Fig 2d: Case 3. Transverse STIR image of the right fore foot showing a high signal subchondral OCLL (arrow) in the distal phalanx at the insertion of the lateral collateral ligament of the DIP joint.

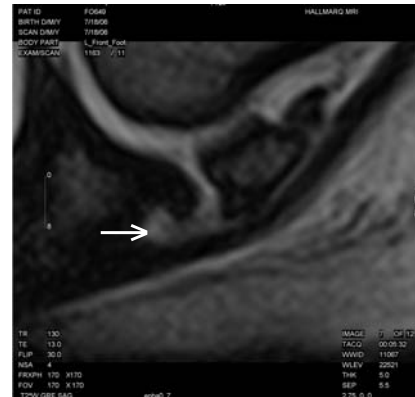


Fig 3b: Case 4. Sagittal GRE T2*-weighted image of the left fore foot showing a high signal OCLL (arrow) in the distal phalanx at the site of insertion of the distal sesamoidean impar ligament.



Fig 2e: Case 3. Frontal (dorsal) GRE T2*-weighted image of the right fore foot showing a high signal subchondral OCLL (arrow) in the distal phalanx at the insertion of the lateral collateral ligament of the DIP joint.

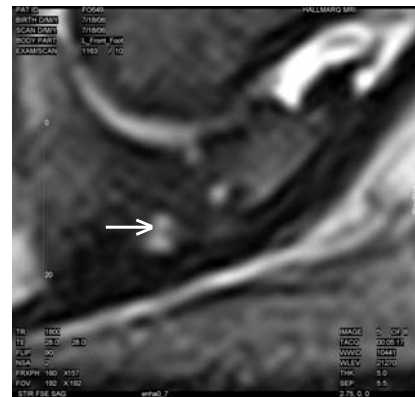


Fig 3c: Case 4. Sagittal STIR image of the left fore foot showing a high signal OCLL (arrow) in the distal phalanx at the site of insertion of the distal sesamoidean impar ligament.

4 feet with OCLLs of the distal phalanx at the site of insertion of one of the collateral ligaments of the DIP joint, the ipsilateral collateral ligament itself demonstrated evidence of desmitis (including enlargement of the ligament and increased T2* signal, and in 2 cases periligamentous high T2* signal).

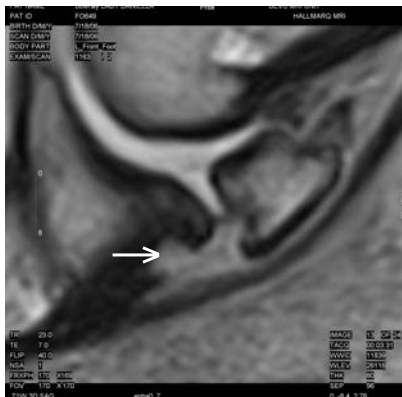


Fig 3a: Case 4. Sagittal GRE T1-weighted image of the left fore foot showing a high signal OCLL (arrow) in the distal phalanx at the site of insertion of the distal sesamoidean impar ligament.

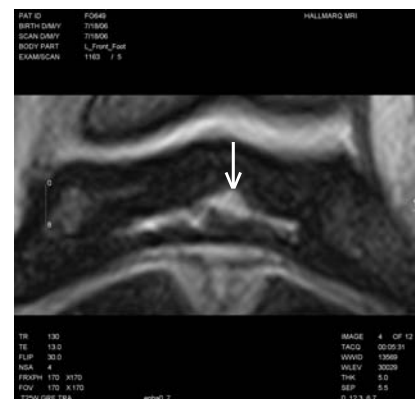


Fig 3d: Case 4. Transverse GRE T2*-weighted image of the left fore foot showing a high signal OCLL (arrow) in the distal phalanx at the site of insertion of the distal sesamoidean impar ligament.

Likewise, in all 3 cases of OCLLs of the distal phalanx at the site of insertion of the distal sesamoidean impar ligament, this ligament itself demonstrated evidence of desmitis (as shown by thickening and lack of definition of the ligament). In the 5 feet with OCLLs identified in the subchondral bone of the DIP joint, significant abnormalities were detected in other



Fig 4a: Case 2. Sagittal GRE T1-weighted image of the left fore foot showing an intermediate signal subchondral OCLL (arrow) in the distal aspect of the middle phalanx. The cyst is surrounded by a rim of decreased signal suggesting osseous sclerosis.



Fig 4c: Case 2. Frontal (dorsal) GRE T2*-weighted image of the left fore foot showing a high signal subchondral OCLL (arrow) in the distal aspect of the middle phalanx. The cyst is seen to communicate with the articular cartilage surface.

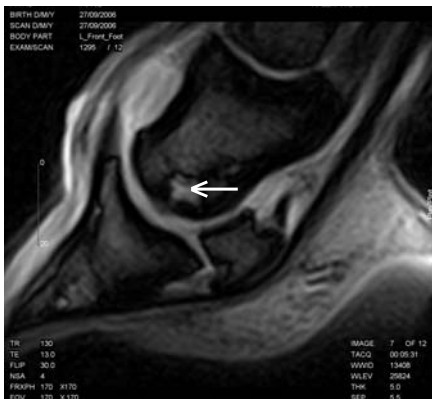


Fig 4b: Case 2. Sagittal GRE T2*-weighted image of the left fore foot showing a high signal subchondral OCLL (arrow) in the distal aspect of the middle phalanx.



Fig 4d: Case 2. Frontal (dorsal) STIR image of the left fore foot showing a high signal subchondral OCLL (arrow) in the distal aspect of the middle phalanx.

structures (including the navicular bone, deep digital flexor tendon, collateral ligaments of the DIP joint, etc).

Re-evaluation of the original foot radiographs following MR imaging enabled 4 OCLLs to be identified in 4 horses (Cases 2, 6, 7 and 9). New radiographic studies using computed radiography allowed radiological identification of a further 4 OCLLs in 2 horses (Cases 3 and 8) (Fig 5). In 2 horses with OCLLs at the site of insertion of the distal sesamoidean impar ligament (Cases 1 and 4) and one horse with a subchondral cystic lesion in the distal phalanx (Case 5), the lesion could not be identified radiologically.

Follow-up information was only available for one horse in this study (Case 6). This horse was subjected to euthanasia and *post mortem* examination confirmed the presence of an OCLL in the subchondral bone of the distal phalanx of the right hind foot (Fig 6). The adjacent articular cartilage showed a focal area of erosion.

Discussion

Standing low-field MR imaging was found to be more sensitive than routine radiography at detecting OCLLs in the feet of these 9 horses. The OCLLs were characterised by well-

demarcated focal high or intermediate signal lesions in all sequences (i.e. GRE T1- and T2*- weighted and STIR images). This MR characteristic is considered to be compatible with either haemorrhage or proteinaceous fluid (Werpy *et al.* 2006). In many of the cysts, the lesion appeared to be surrounded by a rim of osseous sclerosis.



Fig 5: Case 3. Medial dorsoproximal-lateral palmarodistal oblique radiograph of the right fore distal phalanx showing radiolucency (OCLL) (arrow) in the lateral aspect of the bone.

TABLE 3: Major concurrent abnormalities identified by MR imaging in 9 horses with OCLLs of the middle or distal phalanx

Case No.	Fore- or hindlimb	Left	Right
1	Fore	Moderate navicular bone changes (decreased T1 signal in medulla, intermediate STIR signal in medulla, thickened compact bone, increased size of distal synovial fossae) Parasagittal tear in DDFT from level of navicular bone to insertion	Mild navicular bone changes (decreased T1 signal in medulla, thickened compact bone, increased size of distal synovial fossae) DSIL enlarged, irregular in outline and poorly defined
2	Fore	Moderate navicular bone changes (decreased T1 signal in medulla, intermediate STIR signal in medulla)	Severe distension of DIP joint Moderate distension of navicular bursa Moderate navicular bone changes (decreased T1 signal in medulla, intermediate STIR signal in medulla, thickened compact bone, increased size of distal synovial fossae) Swelling and abnormal signal in both collateral ligaments of the DIP joint
3	Fore	Moderately decreased T1 signal throughout medulla of navicular bone Lateral CL enlarged with increased T2* signal	Moderately decreased T1 signal and low STIR signal throughout medulla of navicular bone Lateral CL enlarged with increased T2* signal and increased periligamentous T2* signal
4	Fore	Moderate navicular bone changes (decreased T1 signal in medulla, intermediate STIR signal in medulla, thickened compact bone, increased size of distal synovial fossae) DSIL enlarged, irregular in outline and poorly defined	Moderate navicular bone changes (decreased T1 signal in medulla, intermediate STIR signal in medulla, thickened compact bone, increased size of distal synovial fossae) DSIL enlarged, irregular in outline and poorly defined
5	Fore	Irregular contour of the articular surface of the distal phalanx with irregular signal and thickness of the articular cartilage Parasagittal tear in lateral lobe of DDFT extending from proximal phalanx to navicular bone Moderate distension of navicular bursa Adhesion between dorsal surface of DDFT and CSL	Small core lesion in lateral lobe of DDFT at level of navicular bone DSIL enlarged, irregular in outline and poorly defined
6	Hind	No abnormalities	Severe distension of DIP joint Moderate navicular bone changes (decreased T1 signal in medulla, high STIR signal in medulla)
7	Fore	Moderate navicular bone changes (decreased T1 signal in medulla, intermediate STIR signal in medulla, thickened compact bone, increased size of distal synovial fossae)	Moderate navicular bone changes (decreased T1 signal in medulla, intermediate STIR signal in medulla, thickened compact bone, increased size of distal synovial fossae, modelling of proximal and distal borders) DSIL thickened and poorly defined Navicular bursa moderately distended Medial CL enlarged with increased T2* signal Diffuse decreased T1 signal in medial half of DP
8	Fore	Dorsal irregularity of DDFT at level of CSL and navicular bone Moderate distension of navicular bursa Moderate distension of DIP joint Periarticular modelling of dorsal rim of DIP joint Moderate navicular bone changes (decreased T1 signal in medulla, thickened compact bone, increased size of distal synovial fossae, modelling of proximal and distal borders)	Dorsal irregularity of DDFT at level of CSL and navicular bone Moderate distension of navicular bursa Moderate distension of DIP joint Periarticular modelling of dorsal rim of DIP joint Moderate navicular bone changes (decreased T1 signal in medulla, thickened compact bone, increased size of distal synovial fossae, modelling of proximal and distal borders)
9	Fore	Moderate navicular bone changes (decreased T1 signal in medulla, intermediate STIR signal in medulla, thickened compact bone, increased size of distal synovial fossae) Medial wing of DP has diffusely decreased T1 signal Medial CL enlarged with increased T2* signal and increased periligamentous T2* signal Ossification of the cartilages of the foot	Moderate navicular bone changes (decreased T1 signal in medulla, intermediate STIR signal in medulla, thickened compact bone, increased size of distal synovial fossae) Ossification of the cartilages of the foot Lateral CL enlarged with increased T2* signal

DIP = distal interphalangeal, CL = collateral ligament of the DIP joint, DSIL = distal sesamoidean impar ligament, DDFT = deep digital flexor tendon, CSL = collateral sesamoidean ligament, DP = distal phalanx.

The majority of these OCLLs were in the front feet (11) compared with the hind feet (1), in keeping with previous reports of phalangeal OCLLs (Verschooten and De Moor 1982). The site of the 12 OCLLs diagnosed in the middle and distal phalanges in these 9 horses was fairly equally distributed between the insertion of the collateral ligament of the DIP

joint (4 feet), the insertion of the distal sesamoidean impar ligament (3 feet) and the subchondral bone (5 feet). OCLLs occurring at the site of insertion of the collateral ligament of the DIP joint have been recorded previously. In one study of 18 horses with desmitis of the collateral ligaments of the DIP joint, OCLLs were identified by high-field MR imaging in

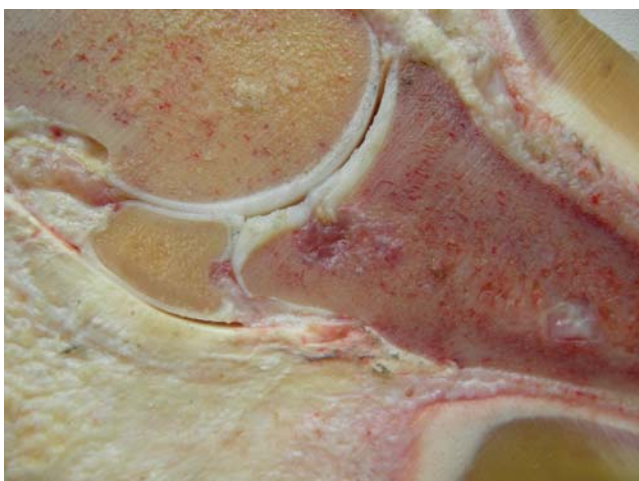


Fig 6a: Case 6. Gross post mortem appearance of the right hind foot (sagittal section) showing the subchondral bone cyst in the distal phalanx. The cyst is surrounded by an area of sclerotic bone.

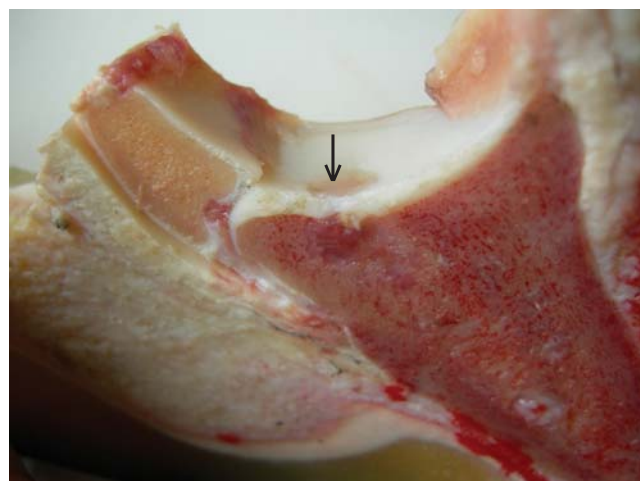


Fig 6b: Case 6. Gross post mortem appearance of the right hind foot (sagittal section) after disarticulation of the DIP joint showing the subchondral bone cyst in the distal phalanx and the overlying erosion of the articular cartilage (arrow).

2 cases (Dyson *et al.* 2004). The precise cause of the cystic change at the insertion of the collateral ligament is uncertain, although it is possible that osteolysis could occur as a result of insertional desmopathy. Histological examination of one case (following surgical debridement and application of a cancellous bone graft) showed ligamentous attachment degeneration associated with osseous resorption and cavitation (Smith *et al.* 2005). Cystic change has also been reported in association with an avulsion fragment of the distal phalanx at the site of insertion of the collateral ligament in one horse (McDiarmid 1998). It was not possible to determine whether the cystic change occurred as a consequence of a primary avulsion fracture of the insertion of the collateral ligament, or was pre-existing and led to the fracture in this horse. A localised area of bone damage of the distal phalanx (without an OCLL) characterised by high MR signal in short tau inversion recovery (STIR) and T2-weighted imaging sequences has also been reported in one other horse in association with desmitis of the collateral ligament (Zubrod *et al.* 2005).

The OCLLs occurring at the site of ligamentous insertions onto the distal phalanx were accompanied by changes affecting the ligaments themselves, confirming the presence of desmitis. The changes in the size and the increase in T2*-weighted signal intensity of the collateral ligaments of the DIP joint in these cases are consistent with inflammation of the soft tissue structure. The distal sesamoidean impar ligament does not necessarily demonstrate this obvious change in T2*-weighting as it differs structurally from the collateral ligament of the DIP joint. Close to its insertion, the distal sesamoidean impar ligament consists of bundles of dense connective tissue adjacent to bundles of vessels and nerve fibres within loose connective tissue septae. The navicular bursa synovial lining (ventrally) and the distal interphalangeal joint synovial lining (dorsally) are attached to the loose connective tissue and can outpouch into the ligament. The presence of OCLLs in association with both desmitis of the collateral ligaments of the DIP joint and desmitis of the distal sesamoidean impar

ligament in the horses in this study is highly suggestive that these osseous lesions occur as a result of an insertional desmopathy. OCLLs have also been recorded at other sites in association with ligamentous and tendinous insertions, including the medial aspect of the proximal radial epiphysis at the site of insertion of the medial collateral ligament of the humeroradial joint (Butler *et al.* 2000; Dyson 2003) and the calcaneus at the insertion of the gastrocnemius tendon (Bassage *et al.* 2000). It is interesting to speculate whether the distal phalanx might be predisposed to OCLL formation secondary to insertional desmopathies as a result of the porous nature of this bone. Unfortunately, none of the cases of OCLLs at the site of ligament insertion in the current series were available for pathological examination of the lesions.

The 5 OCLLs identified in the subchondral bone (4 in the distal phalanx and one in the middle phalanx) appeared to be more typical of the subchondral cystic lesions reported previously in the phalanges and other areas of the body (Pettersson and Sevelius 1968; Jeffcott and Kold 1982; Verschooten and DeMoor 1982; Bertone *et al.* 1986; Specht *et al.* 1988; McIlwraith 1990; Bramlage 1993; Baxter 1996; Textor *et al.* 2001). The aetiopathogenesis of these cysts is uncertain, although it has been suggested that they may develop as a result of defective endochondral ossification, similar to osteochondrosis (McIlwraith 1982; Bramlage 1993). Many of these lesions are diagnosed in young horses (less than 3 years of age), which would support this aetiology. However, in the current cases, all horses with subchondral cystic lesions were older (age range in 4 affected horses 6–17 years). An alternative theory suggests that subchondral cysts may develop secondary to intra-articular trauma, which results in cracks in the articular cartilage that allow synovial fluid to penetrate into the subchondral bone during joint motion, resulting in bone resorption. Intermittent increases in pressure during weightbearing may then result in progressive enlargement of the cyst cavity (Verschooten and DeMoor 1982; Bramlage 1993). This theory would more easily explain the occurrence of

the subchondral cystic lesions in older horses, as seen in this study. The presence of concurrent abnormalities in the ipsilateral and/or contralateral foot shown by MR imaging in all of the horses with subchondral cystic lesions would be supportive of a trauma-associated aetiology. It is possible that other causes of lameness could result in abnormal weightbearing, which subsequently initiates articular cartilage damage. Many of the concurrent lesions identified by MR imaging in the horses in this study are considered likely to be clinically significant (i.e. associated with lameness), since similar lesions are frequently recognised in lame horses but rarely seen in sound horses (Murray *et al.* 2006; Sherlock *et al.* 2007). Sepsis has also been reported to result in subchondral cystic lesions, in the tarsocrural joint, for example (Garcia-Lopez and Kirker-Head 2004), but there was no history or evidence of joint sepsis in any of the horses in this study.

Since all of the horses with OCLLs in this study were found to have other concurrent lesions in their feet, it is impossible to be sure that they contributed to the lameness. However, they were only diagnosed in lame limbs, and were found in the lamest limb in bilaterally lame horses where only one foot had an OCLL, which suggest that the OCLLs were most probably clinically significant. Horses diagnosed with subchondral bone cysts of the distal phalanx are reported to usually be lame, and often have a history of sudden-onset lameness during exercise (Verschooten and DeMoor 1982; Honnas and Trotter 1998).

The pain and lameness associated with subchondral cystic lesions are hypothesised to originate from 2 primary sources: subchondral bone pain associated with increased intraosseous pressure, and synovitis caused by inflammatory debris and mediators shed into the joint (Bramlage 1993). It is interesting to note that in 4 of the 5 DIP joints with subchondral cystic lesions, there was MR evidence of associated joint disease (including moderate or severe synovial distension, periarticular osteophytes or articular cartilage changes), suggesting that persistent inflammation of the joint may have occurred. Various chemical mediators, including neutral metalloproteinases, nitric oxide and prostaglandin E₂, have been shown to be produced by tissue within subchondral bone cysts (Von Rechenberg *et al.* 2000, 2001), and these could be responsible for the development of synovitis and degenerative joint disease.

One of the most surprising features of these cases was the fact that the OCLLs were not diagnosed on initial screening of routine foot radiographs. All of the radiographs were assessed by experienced equine practitioners prior to the horses having MR imaging undertaken. The importance of high-detail radiographs that demonstrate the trabecular pattern of the bone in the affected area in order to identify OCLLs is well-recognised (Watkins 1999). Under-exposed or over-exposed radiographs can underestimate the extent of the lesions or fail to identify them. One reason for traditional radiographs being so difficult to optimise is that x-ray film has a very limited linear response to exposure, requiring fairly narrow and precise exposure factors to produce a truly exceptional radiograph (Mattoon 2006). In areas such as the foot, the variation in size and density of the osseous structures being evaluated, as well as the presence of the

keratinised structures that the beam must pass through mean that a single radiograph cannot produce a high quality image of all areas. This is one reason for 'screening' radiographs not being expected to produce 'diagnostic' information in all areas being imaged. Following the diagnosis of an OCLL by MR imaging, the original radiographs were re-evaluated, and the OCLLs could be identified in 4 horses; the lesions were considered to be subtle and difficult to identify on these original films. This suggests that more careful evaluation of the original radiographs might have permitted the radiological diagnosis of an OCLL to be reached or suspected in at least some cases prior to undertaking MR imaging. However, knowledge of the exact location of the lesion (as determined by MR imaging) was very helpful in aiding the radiological confirmation of the OCLL in these 4 horses; the value of dual diagnostic imaging techniques in diagnosing OCLLs has been recognised previously in other areas, such as the combination of ultrasonography and radiography in the diagnosis of subchondral cystic lesions of the medial femoral condyle (Jacquet *et al.* 2007). In the other 5 horses in this study, OCLLs were still not identified in the original radiographs. In 2 of these horses, further radiographic studies using computed radiography were required in order to identify the cysts radiologically. This demonstrates the value and sensitivity of computed and digital radiography, which allow extensive manipulation of the digital radiographic image (such as window level and width, brightness and contrast), and thereby optimise the identification of subtle lesions (Mattoon 2006). However, computed radiography could still not identify the OCLLs in 3 horses. In addition, most of the concurrent abnormalities identified by MR imaging were not radiologically apparent.

Failure of routine radiography to diagnose OCLLs has been reported previously in the distal phalanx in cases where the lesions were diagnosed by high-field MR imaging (Dyson *et al.* 2004). Likewise, OCLLs of the tarsocrural joint are often not visible on standard radiographs, but may be identified by computed tomography or nuclear scintigraphy (Garcia-Lopez and Kirker-Head 2004). Bone mineral density must change by approximately 30–50% before osseous lesions become radiologically apparent (Butler *et al.* 2000), so small or early cystic lesions may remain undetectable. In addition, the irregular contours of the distal phalanx and the summation of bone densities reflected in conventional radiographs make it unsurprising that OCLLs of the distal phalanx are often not visible radiologically. Nuclear scintigraphy can be helpful in localising OCLLs in some cases, but it lacks the specificity to characterise features such as size, degree of mineralisation and communication with adjacent articulations (Garcia-Lopez and Kirker-Head 2004). Nuclear scintigraphy was not available for use in the horses in this report.

MR imaging is increasingly being employed for diagnosis of the cause of lameness in the distal limb of the horse (Murray and Mair 2005; Werpy *et al.* 2006). A number of recent studies have shown that high-field MR imaging can be an extremely valuable technique for diagnosing pathological changes in the foot (Tucker and Sande 2001; Dyson *et al.*

2003, 2004, 2005). Unfortunately, the expense of high-field MR units limits their use to specialised centres, and the necessity to place the horse under general anaesthesia in order to perform the imaging adds to the costs and risks of the procedure. Recently, a standing low-field MR system, which was used in this study, has become available (Mair *et al.* 2005). Initial results using the low-field standing system to evaluate foot lameness cases have shown a similar range of lesions as has been described using high-field systems (Mair and Kinns 2005; Mitchell *et al.* 2006; Sherlock *et al.* 2007). The results of this study serve to confirm the potential benefits of the system in the evaluation of foot lameness associated with OCLLs in the middle and distal phalanges.

Acknowledgements

The authors thank the referring veterinary surgeons and colleagues at Bell Equine Veterinary Clinic for help with the management of these cases.

Manufacturers' addresses

¹Hallmarq Veterinary Imaging, Guildford, Surrey, UK.

²Fuji Photo Film Ltd, Bedford, UK.

References

- Bassage, L.H., Garcia-Lopez, J. and Currid, E.M. (2000) Osteolytic lesions of the *tuber calcanei* in two horses. *J. Am. vet. med. Ass.* **217**, 710-716.
- Baxter, G.M. (1996) Subchondral cystic lesions in horses. In: *Joint Disease in the Horse*. Eds: C.W. McIlwraith and G.W. Trotter, W.B. Saunders, Philadelphia. pp 384-397.
- Bertone, A.L., McIlwraith, C.W., Powers, B.E., Stashak, T.S., Aanes, W.A. and Turner, T.S. (1986) Subchondral osseous cystic lesions of the elbow of horses: conservative versus surgical treatment. *J. Am. vet. med. Ass.* **189**, 540-546.
- Bramlage, L.R. (1993) Osteochondrosis related bone cysts. *Proc. Am. Ass. equine Practnrs.* **39**, 83-85.
- Butler, J., Colles, C., Dyson, S., Kold, S. and Poulos, P. (2000) The foot, pastern and fetlock. In: *Clinical Radiology of the Horse*, 2nd edn., Eds: J.A. Butler, C.M. Colles, S.J. Dyson, S.E. Kold and P.W. Poulos, Blackwell Scientific, Oxford. pp 27-130.
- Dowling, B.A., Dart, A.J. and Hodgson, D.R. (1998) Subchondral cystic lesions involving the second phalanx in two horses. *Aust. vet. J.* **76**, 328-330.
- Dyson, S.J. (1998) The puzzle of distal interphalangeal joint pain. *Equine vet. Educ.* **10**, 119-125.
- Dyson, S.J. (2003) Radiography and radiology. In: *Diagnosis and Management of Lameness in the Horse*, Eds: M.J. Ross and S.J. Dyson, W.B. Saunders, Philadelphia. pp 153-166.
- Dyson, S.J., Murray, R. and Schramme, M.C. (2005) Lameness associated with foot pain: results of magnetic resonance imaging in 199 horses (January 2001-December 2003) and response to treatment. *Equine vet. J.* **37**, 113-121.
- Dyson, S.J., Murray, R.C., Schramme, M.C. and Branch, M.V. (2003) Magnetic resonance imaging of the equine foot: 15 horses. *Equine vet. J.* **35**, 18-26.
- Dyson, S.J., Murray, R., Schramme, M. and Branch, M. (2004) Collateral desmitis of the distal interphalangeal joint in 18 horses (2001-2002). *Equine vet. J.* **36**, 160-166.
- Garcia-Lopez, J.M. and Kirker-Head, C.A. (2004) Occult subchondral osseous cyst-like lesions of the equine tarsocrural joint. *Vet. Surg.* **33**, 557-564.
- Haack, D., Hertsch, B. and Baez, C. (1988) Zystoide defekte im hufbein des pferdes. *Pferdeheilkunde* **4**, 143-153.
- Honnas, C.M. and Trotter, G.W. (1998) The distal interphalangeal joint. In: *Current Techniques in Equine Surgery and Lameness*, 2nd edn., Eds: N.A. White and J.N. Moore, W.B. Saunders, Philadelphia. pp 389-397.
- Howard, R.P., McIlwraith, C.W. and Trotter, G.W. (1995) Arthroscopic surgery for subchondral cystic lesions of the medial femoral condyle in horses: 41 cases (1988-1991). *J. Am. vet. med. Ass.* **206**, 842-850.
- Jacquet, S., Audigie, F. and Denoix, J.-M. (2007) Ultrasonographic diagnosis of subchondral bone cysts in the medial femoral condyle in horses. *Equine vet. Educ.* **19**, 47-50.
- Jeffcott, L.B. and Kold, S.E. (1982) Clinical and radiological aspects of stifle bone cysts in the horse. *Equine vet. J.* **14**, 40-46.
- Mair, T.S., Kinns, J., Jones, R.D. and Bolas, N.M. (2005) Magnetic resonance imaging of the distal limb of the standing horse. *Equine vet. Educ.* **17**, 74-78.
- Mair, T.S. and Kinns, J. (2005) Deep digital flexor tendonitis in the equine foot diagnosed by low-field magnetic resonance imaging in the standing patient: 18 cases. *Vet. Radiol. Ultrasound* **46**, 458-466.
- Mattoon, J.S. (2006) Digital radiography. *Vet. Comp. orthop. Traumatol.* **19**, 123-132.
- McDiarmid, A.M. (1998) Distal interphalangeal joint lameness in a horse associated with damage to the insertion of the lateral collateral ligament. *Equine vet. Educ.* **10**, 114-118.
- McIlwraith, C.W. (1982) Subchondral cystic lesions (osteochondrosis) in the horse. *Comp. cont. Educ. pract. Vet.* **4**, S394-S404.
- McIlwraith, C.W. (1990) Subchondral cystic lesions in the horse - the indications, methods and results of surgery. *Equine vet. Educ.* **2**, 75-80.
- Mitchell, R.D., Edwards, R.B., Makkreel, L.D. and Oliveira, T.D. (2006) Standing MRI lesions identified in jumping and dressage horses with lameness isolated to the foot. *Proc. Am. Ass. equine Practnrs.* **52**, 422-426.
- Murray, R.C. and Mair, T.S. (2005) The use of magnetic resonance imaging in lameness diagnosis in the horse. *In Pract.* **27**, 138-146.
- Murray, R.C., Schramme, M.C., Dyson, S.J., Branch, M.V. and Blunden, T.S. (2006) Magnetic resonance imaging characteristics of the foot in horses with palmar foot pain and control horses. *Vet. Radiol. Ultrasound* **47**, 1-16.
- Pettersson, H. and Sevelius, F. (1968) Subchondral bone cysts in the horse: a clinical study. *Equine vet. J.* **1**, 75-80.
- Scott, E.A., Snyder, S.P., Schmotzer, W.B. and Pool, R. (1991) Subchondral bone cysts with fractures of the extensor processes in a horse. *J. Am. vet. med. Ass.* **199**, 595-597.
- Sherlock, C.E., Kinns, J. and Mair, T.S. (2007) Evaluation of foot pain by low field magnetic resonance imaging in the standing horse: results in 41 cases with long-term follow-up. *Vet. Rec.* In Press.
- Smith, M.R.W., Crowe, O.C., Ellson, C., Turner, S.J., Patterson-Kane, J.C., Schramme, M.C. and Smith, R.K.W. (2005) Surgical treatment of osseous cyst-like lesions in the distal phalanx arising from collateral ligament insertional injury. *Equine vet. Educ.* **17**, 195-200.
- Specht, T.E., Nixon, A.J., Colahan, P.T., Moore, B.D. and Brown, M.P. (1988) Subchondral cyst-like lesions in the distal portion of the radius in four horses. *J. Am. vet. med. Ass.* **193**, 949-952.
- Story, M.R. and Bramlage, L.R. (2004) Arthroscopic debridement of subchondral bone cysts in the distal phalanx of 11 horses (1994-2000). *Equine vet. J.* **36**, 356-360.

- Textor, J.A., Nixon, A.J., Lumsden, J. and Ducharme, N.G. (2001) Subchondral cystic lesions of the proximal extremity of the tibia in horses: 12 cases (1983-2000) *J. Am. vet. med. Ass.* **218**, 408-413.
- Tucker, R.L. and Sande, R.D. (2001) Computed tomography and magnetic resonance imaging in equine musculoskeletal conditions. *Vet. Clin. N. Am.* **17**, 145-157.
- Verschooten, F. and De Moor, A. (1982) Subchondral cystic and related lesions affecting the equine pedal bone and stifle. *Equine vet. J.* **14**, 47-54.
- Von Rechenberg, B., Leutenegger, C., Zlinsky, K., McIlwraith, C.W., Akens, M.K. and Auer, J.A. (2001) Upregulation of mRNA of interleukin-1 and -6 in subchondral cystic lesions of four horses. *Equine vet. J.* **33**, 143-149.
- Von Rechenberg, B., Guenther, H., McIlwraith, W.C., Leutenegger, C., Frisbie, D.D., Akens, M.K. and Auer, J.A. (2000) Fibrous tissue of subchondral cystic lesions in horses produce local mediators and neutral metalloproteinases and cause bone resorption *in vitro*. *Vet. Surg.* **29**, 420-429.
- Wagner, P.C., Modransky, P.D., Gavin, P.R. and Grant, B.D. (1982) Surgical management of subchondral bone cysts of the third phalanx in the horse. *Equine Pract.* **4**, 9-15.
- Watkins, J.P. (1999) Osteochondrosis. In: *Equine Surgery*, 2nd edn., Eds: J.A. Auer and J.A. Stick. W.B. Saunders, Philadelphia. pp 765-778.
- Werpy, N.M., Ho, C.P., Kawcak, C.E., Rantanen, N.W. and McIlwraith, C.W. (2006) Review of principles and clinical applications of magnetic resonance imaging in the horse. *Proc. Am. Ass. equine Practns.* **52**, 427-440.
- Zubrod, C.J., Schneider, R.K., Tucker, R.L., Gavin, P.R., Ragle, C.A. and Farnsworth, K.D. (2004) Use of magnetic resonance imaging for identifying subchondral bone damage in horses: 11 cases (1999-2003). *J. Am. vet. med. Ass.* **224**, 411-418.
- Zubrod, C.J., Farnsworth, K.D., Tucker, R.L. and Ragle, C.A. (2005) Injuries of the collateral ligaments of the distal interphalangeal joint diagnosed by magnetic resonance. *Vet. Radiol. Ultrasound* **46**, 11-16.